Self-Assembled Monolayers of Disulfide-Functionalized Diacetylenes on Gold Films and Nanoparticles

ARTICLE *in* THE JOURNAL OF PHYSICAL CHEMISTRY C · DECEMBER 2006

Impact Factor: 4.77 · DOI: 10.1021/jp0640777

8 AUTHORS, INCLUDING:

Anna Demartini
Università degli Studi di Genova
18 PUBLICATIONS **103** CITATIONS
SEE PROFILE

Sergio Thea
Università degli Studi di Genova
95 PUBLICATIONS **782** CITATIONS
SEE PROFILE

Emilia Giorgetti
Italian National Research Council
136 PUBLICATIONS **801** CITATIONS
SEE PROFILE

Giovanna Dellepiane
Università degli Studi di Genova
213 PUBLICATIONS **1,953** CITATIONS
SEE PROFILE

Self-Assembled Monolayers of Disulfide-Functionalized Diacetylenes on Gold Films and Nanoparticles

Marina Alloisio,[†] Anna Demartini,[†] Carla Cuniberti,[†] Giovanni Petrillo,[†] Sergio Thea,[†] Emilia Giorgetti,[‡] Anna Giusti,[†] and Giovanna Dellepiane*,[†]

INSTM and Dipartimento di Chimica e Chimica Industriale, Università di Genova, Via Dodecaneso 31-16146 Genova, Italy, and INSTM and Istituto dei Sistemi Complessi−CNR, Via Madonna del Piano 10-50019 Sesto Fiorentino (Firenze), Italy

Received: June 29, 2006; In Final Form: October 23, 2006

This paper reports on the fabrication of self-assembled monolayers containing disulfide-functionalized diacetylenes. To this purpose, two diacetylene derivatives were synthesized: the novel 14-(9*H*-9-carbazolyl)-tetradeca-10,12-diyn-1-yl disulfide (CDS9) and the henicosa-10,12-diyn-1-yl disulfide (DS9). Both monomers were employed to prepare two-dimensional self-assembled monolayers (2D-SAMs) by chemisorption on gold-sputtered platforms and three-dimensional self-assembled monolayers (3D-SAMs) on gold nanoclusters by direct synthesis in organic solvent. The chemisorbed diacetylenes were then converted to the polymeric form by exposure to UV radiation, and their morphological and spectroscopic properties investigated by several techniques. From SERS data it was inferred that both monomers show the same behavior, in that the highly conjugated blue phase was observed in the 3D-SAMs, while only the less extended red conformation was found in the corresponding 2D-SAMs.

Introduction

The development of properly designed systems is necessary to meet the demand for materials to be used in all-optical signal processors and sensing devices. This requirement has guided our recent work on the preparation of functional materials based on substituted diacetylenes suitable for obtaining hybrid metal/organic nanostructures. The choice of the diacetylene moiety has been dictated by several reasons. Among conjugated polymers the polydiacetylenes (PDA), which are obtained by a topochemical polymerization of the monomers, show one of the largest values for the nonresonant optical nonlinearity in the subpicosecond time regime.[1] Our experience has developed in the synthesis and the physical and optical characterization of a particular class of polydiacetylenes (the polycarbazolyldiacetylenes, PCDA) having electron donor carbazolyl groups as substituents.[2] The presence of the carbazolyl groups makes these materials attractive for their hole-transporting, photoconducting, and enhanced nonlinear optical properties.[3−5] Extended literature data on self-assembled monolayers of diacetylene disulfides on gold have shown the formation of robust polymeric chains with promising optoelectronic behavior.[6,7] Moreover, the measurement of the third-order susceptibility $\chi^{(3)}$ performed by surface plasmon spectroscopy on a quasi-monomolecular layer of a soluble PCDA spun on silver-coated plates gave a very large off-resonance nonlinearity ($\chi^{(3)} \sim 10^{-8}$ to 10^{-9} esu at 1064 nm with picosecond pulses).[8−10] The giant nonlinearity observed and related to the nanostructured surface of the silver film, providing an e.m. mechanism for the enhancement of the nonlinearity through local field effects,[11] makes these hybrid structures outstanding for application in devices having photonic band gap properties.[12] On the basis of these data we have synthesized a novel carbazolyldiacetylene monomer, the 14-(9*H*-9-carbazolyl)tetradeca-10,12-diyn-1-yl disulfide, hereafter named CDS9, properly designed to ensure a stable anchoring to the metal substrate through the S−Au bond. For the sake of comparison, we have also prepared the diacetylene monomer dihexacosa-7,9-diyn disulfide, hereafter named DS9.[6]

The polymerization behavior of diacetylene compounds is usually monitored using UV−vis absorption spectroscopy. In fact, while diacetylene monomers are transparent in the visible region, the polymers present strong colored forms corresponding to the so-called red and blue phases, the absorption maxima of which are centered at about 540 and 640 nm, respectively. However, this technique is not useful for studying monolayer assemblies on gold because of the very low absorbance of the PDA monolayer and of the spectral overlap arising from the substrate plasmon bands.

Raman spectroscopy provides a good alternative approach for detecting the polymerization of diacetylenes and the type of the conjugated polymeric form.[13,14] It is well-known, indeed, that the resonance-enhanced vibrational modes of the conjugated backbone corresponding to the stretchings of the triple and double bonds in the polymer originate peaks at about 2080 and 1450 cm^{-1}, respectively, for the "more conjugated" blue form and at about 2100 and 1500 cm^{-1} for the "less conjugated" red one. These frequencies, considerably lower than those of the isolated triple and double bonds (around 2260 and 1620 cm^{-1}), give a direct evidence of the polymer formation.

Also surface enhancement effect, besides Raman resonance, can contribute to the observation of polydiacetylene modes in monolayers on a rough Ag or Au surface. In this case, different selection rules are operative and the enhancement favors the vibrational modes occurring normally to the surface. Surface-enhanced Raman spectroscopy (SERS) is then a useful tool for investigating monolayers, and sometimes both resonant and surface contributions are present.

In this paper we will describe the synthesis of CDS9, the fabrication of self-assembled monolayers (SAMs) by chemi-

[†] INSTM and Università di Genova.
[‡] INSTM and Istituto dei Sistemi Complessi−CNR.

10.1021/jp0640777 CCC: $37.00
Published on Web 12/06/2006

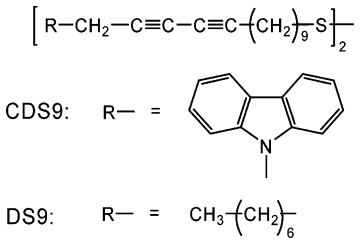

Figure 1. Chemical structures of diacetylene disulfides CDS9 and DS9.

sorption of both monomers on gold surfaces of different geometry, their photochemical polymerization, and the characterization of the polymer monolayers. In order to investigate the influence of the constraints of the substrate size and shape on the molecular coverage and on the polymerization process, we prepared two-dimensional (2D) SAMs on gold-sputtered platforms and three-dimensional (3D) SAMs on gold colloids. That thiol-substituted Au clusters can be regarded as three-dimensional analogs of self-assembled monolayers formed by the same thiol-substituted ligands on flat Au surfaces is well recognized.[15−17] In particular, we will present for the first time the direct synthesis of diacetylene-capped gold nanoparticles in organic solvents through a modified version of the Brust method.[18] Previous works on chemisorbed diacetylenes onto gold colloids were based on the use of preformed nanoclusters.[19,20]

Experimental Methods

Materials and Synthesis. The CDS9 monomer (Figure 1) was obtained according to the route sketched in Scheme 1. The detailed synthetic procedure is reported in the Appendix, together with the full characterization of CDS9 as well as of all the intermediates which were not reported previously in the literature. The DS9 monomer, synthesized according to the procedure described in ref 21, showed analytical and spectroscopic data in full agreement with those reported therein. The purity of the final monomers was also assessed by HPLC−UV−DAD chromatography. ^{1}H and ^{13}C NMR spectra are reported as supplementary material in the Supporting Information, together with the HPLC trace of CDS9.

All chemical reagents and spectroscopic-grade solvents were commercial products used as received except when anhydrous conditions were required. The gold salt $AuCl_3$, $NaBH_4$, and trisodium citrate were purchased from Lancaster. MilliQ water was used for all aqueous solutions.

Column chromatographies were carried out on Merck Kieselgel 60 silica gel, and melting points were determined on a Buchi 535 apparatus.

Photopolymerization of diacetylenes was carried out in a Rayonet photochemical chamber reactor, operating at 254 nm and 35 W power. The samples were kept at 10 cm distance from the UV lamps.

HPLC. Instrument and conditions: Agilent 1100 equipped with a DAD detector; column, Hypersil MOS RP C8 100 mm × 2.1 mm, particle size 5 μm, flow 300 μL/min; eluents, (A) H_2O−AcOH (0.2%); (B) MeOH−AcOH (0.2%). Linear gradient (B%): 0 min, 50%, 10 min, 100%. Temperature: 30 °C

MS Spectrometry. An Agilent MSD Ion Trap Classic, positive-ion electrospray mode, was used.

NMR Spectroscopy. ^{1}H and ^{13}C NMR spectra were taken on a Varian Gemini 300 spectrometer; TMS was used as internal standard.

SCHEME 1: Synthetic Route to CDS9[a]

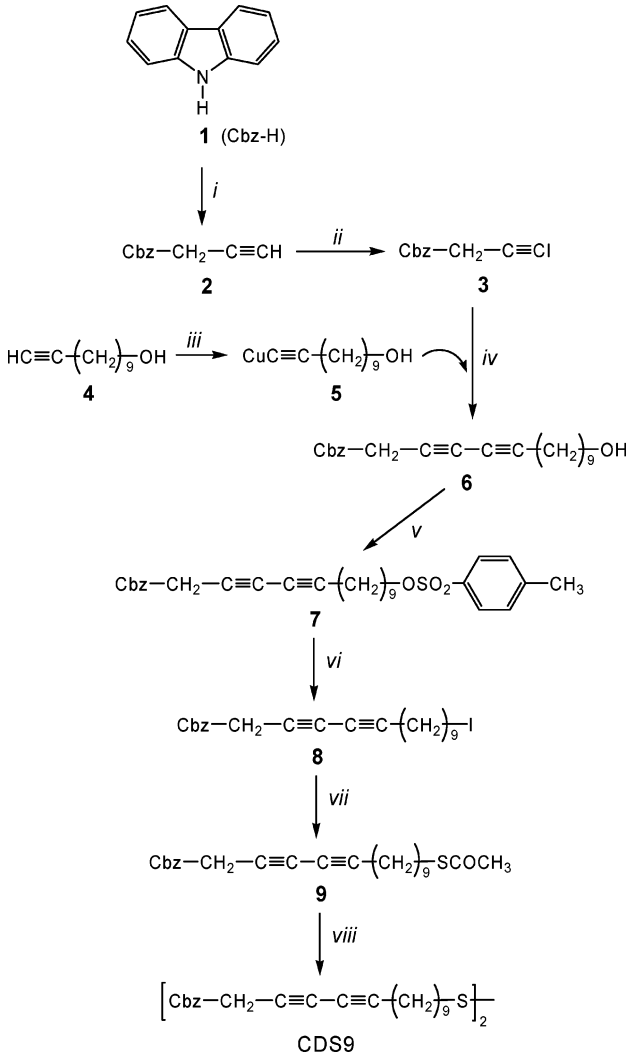

[a] (i) Propargyl bromide, NaOH, Bu_4NI, H_2O/toluene; (ii) *n*-BuLi, I_2, THF; (iii) CuCl, NH_3/$HONH_3Cl$/EtOH; (iv) pyridine; (v) *p*-tosylchloride, pyridine; (vi) NaI, acetone; (vii) CH_3COSK, DMF; (viii) KOH/acetone.

UV−Vis Spectroscopy. Electronic absorption spectra were recorded at room temperature on a Perkin-Elmer Lambda 9 spectrophotometer.

Fluorescence Spectroscopy. Emission spectra were performed at 25 °C with a Perkin-Elmer MPF-44A spectrofluorimeter. Emission intensities from excitation at different wavelengths were normalized at a constant value of the source intensity.

Raman Spectroscopy. MicroRaman spectra were collected using a Renishaw System 2000 equipped with a Leica microscope (633 nm line of He−Ne laser, 1−16 accumulations, 50% or 100% power, 50×) in the range of 2500−600 cm^{-1}. Raman spectra were recorded using a Jobin-Yvon HG2S monochromator equipped with a cooled RCA-C31034A photomultiplier (514.5 nm line of an Ar^+ laser).

Optical Microscopy. Optical images were acquired using a Leica IM microscope, model DM 4000 M, equipped with Leica DC photocamera and Qwin software V3 for digital image processing and analysis.

Transmission Electron Microscopy. Bright-field images were obtained with a Jeol electron microscope, model IEM-2010, operating at 200 kV. Specimens were prepared by evaporating a drop on a 300 mesh carbon-coated copper grid

TABLE 1: Synthesis Conditions and Average Dimensions for Stabilized AuNPs

sample	$HAuCl_4$ mM	ligand/$HAuCl_4$ molar ratio	$NaBH_4$/$HAuCl_4$ molar ratio	NP diameter (nm)
CDS9	4.6	1:2	10:1	4.5
				21.0
DS9	4.6	1:1	1:1	7.5
$C_{12}H_{23}SH$		1:2	10 :1	1.6
$C_{12}H_{23}SH$		1:1	1:1	5.4

(Lacey). Qwin software V3 for digital image processing and analysis was used for the measurement of particle size, employing multiple pictures from different areas.

Sample Preparation. SAMs of CDS9 and DS9 were fabricated on both gold platforms and colloidal nanoparticles, successively deposited on quartz or glass microscope slides.

The substrates were previously cleaned by sonication with H_2O MilliQ, acetone, and hexane and afterward treated with boiling piranha solution (7:3 v/v H_2SO_4/H_2O_2) for 1 h. In order to help the metal anchoring to the SiO_2 surfaces, an adhesive layer was established on the slides by immersion in a 2% v/v solution of (3-mercaptopropyl)trimethoxysilane (MPTS) in ethanol for 4 h.

Diacetylene SAMs on Gold Platforms (2D-SAMs). Sputtered gold layers on functionalized silica substrates were prepared using an electrical discharge deposition system (SEM coating unit PS3 from Agar Aids for Electron Microscopy). Au films of about 20 nm thickness were obtained and immediately immersed in a 1 mM chloroform solution of the diacetylene disulfides. After 48 h of equilibration at room temperature, the samples were removed and thoroughly rinsed with spectroscopic-grade chloroform in order to dissolve the excess monomer deposited and then dried in air. Strict light control was maintained during preparation and storage of diacetylene solutions and monolayer films to avoid the possibility of spurious polymerization. The resulting diacetylene monolayers were subsequently polymerized by UV irradiation.

Diacetylene SAMs on Gold Colloidal Nanoparticles (3D-SAMs). Diacetylene-stabilized gold nanoparticles (AuNP) were prepared by a modified version of the Brust method[18] as described by Hoestetler et al.[22] Different preparation conditions were set up for the two disulfides, as shown in Table 1. The $NaBH_4$ reducing agent was delivered in about 10 s, and the reaction was allowed to complete under vigorous stirring at room temperature for 5 h. By this way, quite stable deep purple toluene solutions were obtained for DS9-protected AuNPs (Figure 2a), but not for the CDS9/AuNP system, due to the very low solubility of the CDS9 disulfide in the solvent. In this case, by adding the reducing aqueous solution of $NaBH_4$ to an organic suspension containing $HAuCl_4$ and the diacetylene monomer, a deep purple precipitate at the H_2O/toluene interface could be observed, composed by gold nanoparticles capped with CDS9 (Figure 2b). The precipitate was isolated and partially solubilized with chloroform, a better solvent for the monomer.

Owing to the different solubility of CDS9 and DS9 disulfides in organic solvents, two different procedures were followed to deposit the diacetylene-derivatized gold nanoparticles on glass and quartz slides, previously thiol-functionalized as described above. Films of DS9-coated AuNPs were obtained by dipping the substrate into the corresponding toluene solution and allowing the solvent to completely evaporate, while films of CDS9-coated AuNPs were fabricated by simple casting of the nanoparticle suspension in chloroform onto the functionalized silica surface. As prepared, the samples were rinsed with spectroscopic-grade solvent, dried in air, and then photopolymerized in the Rayonet reactor.

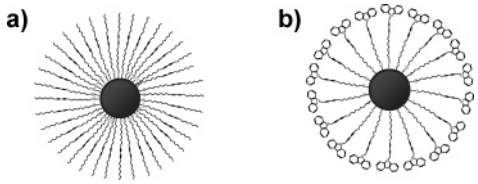

Figure 2. Schematic representation of gold nanoparticles (AuNPs) capped with DS9 (a) and CDS9 (b).

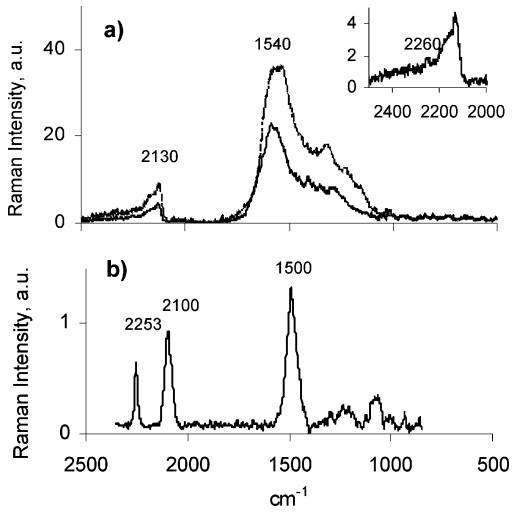

Figure 3. (a) SERS spectra of SAM of polyCDS9 chemisorbed on sputtered gold film after 7 min of UV irradiation (Au absorption background subtracted). Laser excitation at 514.5 nm (lower) and 633 nm (upper). (b) SERS spectra of SAM of polyDS9 chemisorbed on sputtered gold film after 20 min of UV irradiation. Laser excitation at 514.5 nm.

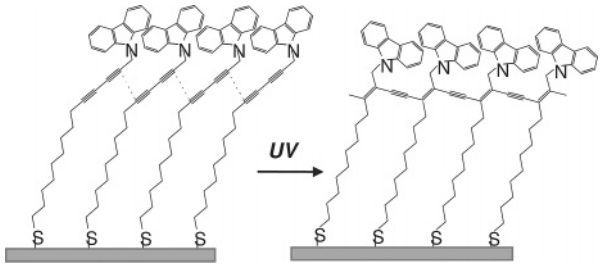

Figure 4. Polymerization scheme of CDS9 SAM on sputtered gold film; the dotted lines in the left image show the steric requirements for the polymerization process.

Results and Discussion

Diacetylene SAMs on Gold Platforms (2D-SAMs). Figure 3 reports the Raman spectra of photoirradiated CDS9 and DS9 monolayers on Au recorded using the 633 and 514.5 nm exciting lines. At both excitations, the spectrum of polyCDS9 (Figure 3a) exhibits signals at 2100 and around 1500 cm^{-1} typical of the red form of the polymer, the latter showing a broadening not observed for other PDA monolayers.[6] By taking into account the surface effect and the SERS selection rules, these spectral features can be interpreted on the basis of the polymer assembly architecture depicted in Figure 4, where both the double bond and the carbazolyl rings are nearly perpendicular to the metal/polymer interface, while the triple bond is almost parallel to it. Because of the monolayer structure, peaks due to the double-bond stretching vibrations of the aromatic rings are present and overlap the polymer double-bond signal giving rise to the broad feature in the 1500−1200 cm^{-1} range. A shoulder is observed

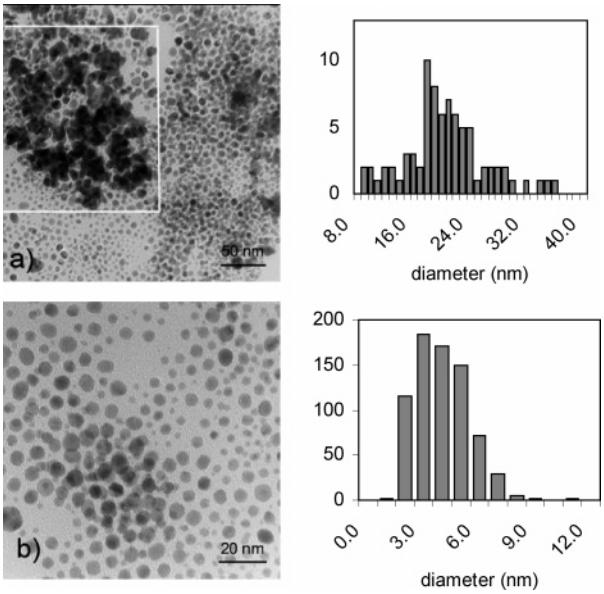

Figure 5. (a) Bright-field TEM image obtained from a AuNP/CDS9 chloroform solution and histogram of the particle size distribution related to the delimited area. (b) Enlarged TEM image of smaller AuNP/CDS9 particles of part a and the corresponding histogram of the particle size distribution.

in the high-frequency region of the triple bonds (see inset in Figure 3a) which can be attributed to monomer residues still present. Sharp peaks at 2100 and 1500 cm^{-1}, typical of the red form of the polymer, are observed in the spectrum (here reported only at 514.5 nm) of the photoirradiated DS9 monolayer on Au (Figure 3b). The evident monomer peak at 2253 cm^{-1} indicates that, despite the prolonged UV exposure time, unpolymerized material is still present. Here, the relative intensity of the 1500 cm^{-1} signal to that at 2100 cm^{-1}, substantially lower than for polyCDS9, can be interpreted in terms of a structure similar, though a little more distorted, to that in Figure 4. The weak, low-resolved features between 700 and 1400 cm^{-1} are not definitely assigned in the literature but can be reasonably associated with collective modes of the alkylic chain. We would like to stress that for both polymers on Au films no evidence of the blue form is found, while for photopolymerized CDS9 monolayers on silver coatings of different roughness[23,24] both red and blue phases were found to coexist. The fact that in our conditions only the red polymer is obtained also from SAMs of DS9, which is known to easily polymerize in the blue or red form as a function of the fabrication method and in particular of the substrate preparation,[25] indicates in the substrate morphology the dominant factor.

Diacetylene SAMs on Gold Colloidal Nanoparticles (3D-SAMs). An alternative method of diacetylene SAM fabrication based on the direct synthesis of nanosized gold colloids capped with monomers was set up as described in Experimental Methods. The resulting organic-protected gold nanoassemblies were morphologically and spectroscopically analyzed both as colloidal suspensions and after deposition on properly functionalized silica slides.

TEM micrographs of drop-cast films of AuNP/CDS9 chloroform solutions and of AuNP/DS9 toluene solutions are presented in Figures 5 and 6, respectively. Corresponding histograms of the particle size distributions are reported alongside. The resulting average values of NP diameter are listed in Table 1. The sample of Figure 5a exhibits a wide dispersion in size and shape. Irregular aggregates, essentially composed of relatively large particles (21 nm mean diameter), are present

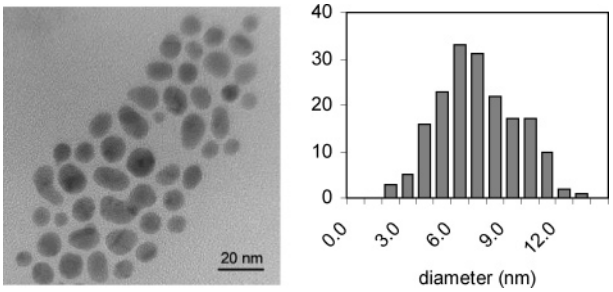

Figure 6. Bright-field TEM image and histogram of the particle size distribution obtained from a AuNP/DS9 toluene solution.

in a quite broad size distribution, as revealed by the histogram related to the area delimited by the white lines. The aggregates coexist together with small near-spherical particles of about 4.5 nm diameter, the characteristics of which are better pointed out in Figure 5b. Where agglomeration is not present, the particles form a 2D structure, in which the closest core−core spacing is approximately equal to the estimated length of the half-moiety of CDS9 (2.2 nm).[23,26] The tendency to form self-assembled ordered superlattices observed for alkanethiol-capped nanoclusters[27] was explained by means of intercalation or interdigitation of alkyl chains, conformation defects, or chain bundles of adjacent cluster molecules.[22]

A more homogeneous pattern, where well-separated spherical (prevalent) and elongated DS9-stabilized AuNPs are visible, is shown in Figure 6. The axial ratio is ranging from 1 to 2, and the diameter distribution is reasonably narrow, peaked at 7.5 nm. Also in this case the particles arrange into an ordered array in which the least intercore distance of about 3 nm corresponds to the DS9 disulfide half-moiety extended length. It is worth noting, however, that for both samples the distance between two clusters is often much larger than one chain length and voids are also present, reflecting a significant degree of packing disorder in the nanocrystalline structure.

The two types of nanoparticles exhibit discernible variety of particles size and disposition, due to the differences in the chemical nature of the ligand shell surrounding the metallic core as well as in the synthesis protocol. In fact, it is well-known that the manipulation of the preparative reaction conditions produces changes in cluster dimensions.[18,22,28]

In order to clarify the influence of the synthetic procedure on the particle morphology, dodecanethiolate-stabilized Au clusters, a fully investigated organic-capped metallic system, were prepared according to the concentrations in Table 1. The average dimensions of the resulting nanoparticles, measured from the TEM images (shown in the Supporting Information) are also reported in Table 1. The values result lower than those found for the diacetylene-derivatized systems prepared in the same operative conditions, in particular for the higher $NaBH_4$/Au ratio, so indicating that not only the synthesis protocol, but also the chemical properties of the chemisorbed ligand are important in determining the nanocluster size and shape.

Alternative efficient tools for investigating the state of organic-coated AuNPs are represented by electronic absorption and emission spectroscopies. It is well-established that the UV−vis spectra of gold nanoparticles are characterized by the presence of a strong absorption peak, ascribed to the surface plasmon resonance (SPR),[29] known to be strongly dependent on the metallic cluster size and shape[22,28] and also sensitive to the surface-adsorbed species and dielectric constant of the medium.[29,30] In comparison with the investigations done on the surface plasmon absorption band, studies on the photoluminescence of AuNPs are quite limited.[31−37] Like the absorption

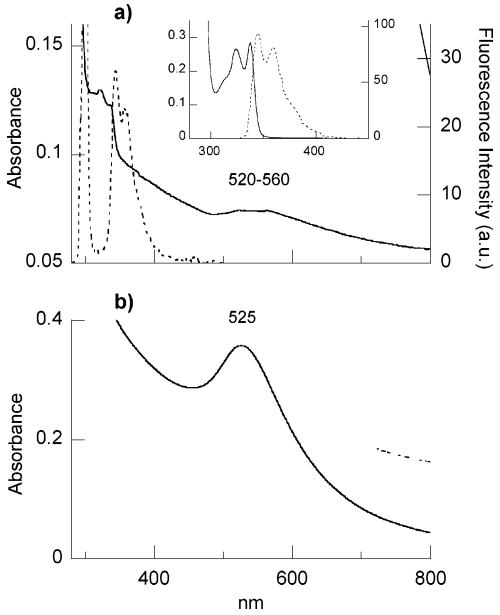

Figure 7. (a) Electronic absorption (solid line) and fluorescence (dotted line) spectra of chloroform solutions of AuNPs capped with CDS9 and of free CDS9 (inset). Excitation wavelength = 300 nm. (b) Electronic absorption spectrum of a toluene solution of AuNPs capped with DS9 diacetylene.

properties, the photoluminescence of gold nanoclusters is also strongly influenced by their size and shape[31,38] as well as by the nature of the organic ligand shell.[33]

Electronic absorption and fluorescence studies were carried out on CDS9- and DS9-capped gold nanoclusters dispersed in solvents in order to confirm the morphological indications achieved by TEM analysis. The absorption and fluorescence spectra of a CDS9/AuNP chloroform solution and the absorption spectrum of a DS9/AuNP toluene solution are reported in Figure 7, parts a and b, respectively, together with the spectra of the free CDS9 diacetylene ligand in the same solvent (inset). In Figure 7a a broad surface plasmon peak with maximum extending from 520 to 560 nm is observed. The plasmon absorbance, responsible for the pink-violet color of the colloidal solution, is typical of nanosized gold clusters. As NP aggregation leads to a broadening and red-shifting in the SP shape, the band breadth suggests the presence in solution of particles of variable dimensions. Nevertheless, the absence of the longitudinal plasmon resonance band[29] in the 650−700 nm range indicates that in this sample the aggregation degree is quite low and very asymmetric assemblies are not formed. In the near-UV region, the two weak signals at 322 and 336 nm, superimposed upon a continuous rising background, are related to the intense and well-defined doublet at 344 and 356 nm in the fluorescence spectrum described by the dashed curve. These spectral features, that resemble those of the free CDS9 monomer in chloroform solution (inset of the figure), can be assigned to the absorption and emission transitions of the carbazolyl end-groups. Notice that no evidence of intrinsic fluorescence of metal cores can be detected.

On the whole, spectroscopic data and TEM images indicate that modestly dispersed, nearly spherical nanosized Au clusters coated with CDS9 diacetylene were fabricated.

The spectrum of Figure 7b, related to DS9-capped AuNPs in toluene solution, displays a distinct and intense surface plasmon band around 525 nm, the rather narrow profile of which confirms the higher size/shape homogeneity of the nanoclusters already evidenced by means of TEM investigation. In this case

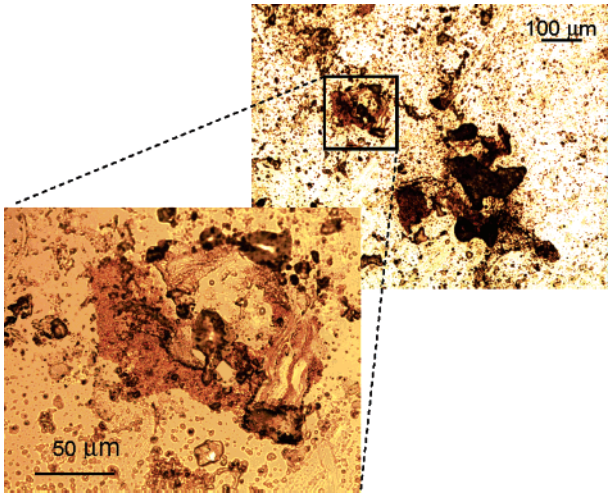

Figure 8. Optical images at different magnifications of a AuNP/CDS9 film on thiol-functionalized glass substrate.

no luminescence emission from the sample could be detected. It is evident that the overall spectral behavior agrees with the synthesis of homogeneous gold nanoparticles protected with a monolayer of adsorbed DS9 chains.

In conclusion, spectroscopic investigations on the organic-capped metallic nanohybrids prepared in this work show that the electronic spectra of these systems are almost independent of the adsorbed chain nature and length, but very sensitive to the core mass, and as a consequence, they confirm that it is possible to tune the optical properties of these materials by altering the particle dimensions.[39]

Films of Diacetylene-Capped AuNPs. Attempts to study the photopolymerization in solution of CDS9 and DS9 chemisorbed on gold colloids were made, but so far without satisfactory results. UV−vis spectroscopy, in the presence of intense gold surface plasmon bands, turned out to be not very sensitive in discriminating typical polydiacetylene absorptions (data not shown). As a consequence, a direct comparison of the morphological and optical properties between 2D- and 3D-SAMs of the two monomers could not be performed. In order to overcome this inconvenience, diacetylene-coated AuNPs were immobilized onto properly thiol-functionalized silica slides, following the procedure described in Experimental Methods. The morphology of the films was analyzed by optical microscope, and spectroscopic properties were studied by several techniques (UV−vis, fluorescence, SERS). The samples were then irradiated at 254 nm for different times and then investigated by means of SERS spectroscopy at the 633 nm laser excitation line.

Figure 8 displays the optical images of a film of CDS9-stabilized AuNPs cast on a MPTS-derivatized quartz substrate. Dark large disordered aggregates of area ranging from 400 to 7000 μm^2 and formed by particle coagulation are clearly visible. The related electronic absorption spectrum (Figure 9, solid line) is consistent with the presence of an irregular cluster self-assembly, in that the spectral profile looks noisy and rather undefined with the broad plasmon band about 20 nm red-shifted with respect to the corresponding chloroform solution. In any case, very weak but still detectable carbazole absorptions are recognizable around 330 and 340 nm as well as the corresponding emission peaks (dotted line) at higher wavelengths (about 350 and 360 nm).

Quite different is the topography of the DS9-capped nanoparticle film, shown in Figure 10. Compact two-dimensional islands of quite irregular form and of area ranging from 40 to 70 μm^2 cover uniformly but not completely the substrate

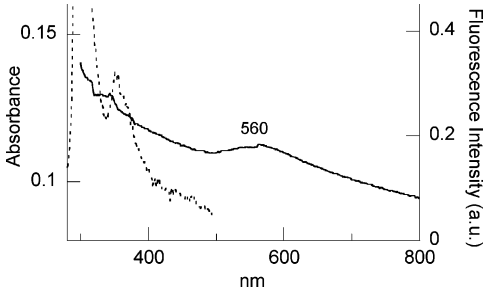

Figure 9. Electronic absorption (solid line) and fluorescence (dotted line) spectra of AuNPs capped with CDS9 deposited onto a functionalized glass slide. Excitation wavelength = 300 nm.

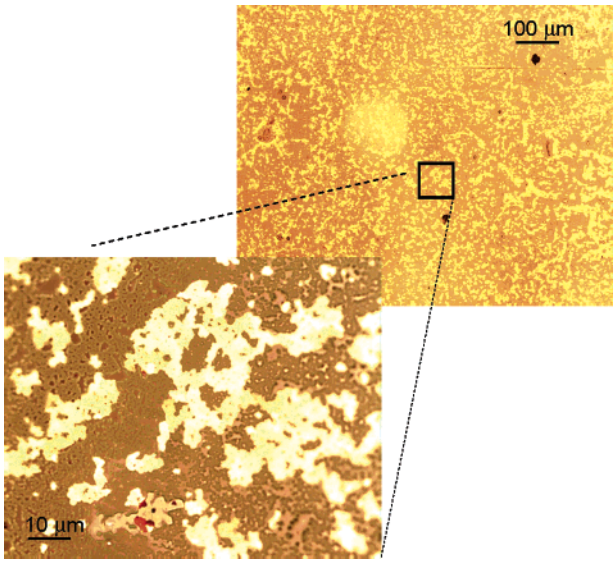

Figure 10. Optical images at different magnifications of AuNP/DS9 film on thiol-functionalized quartz substrate.

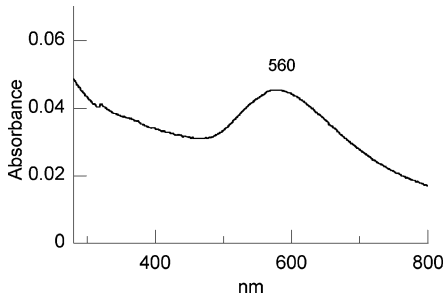

Figure 11. Electronic absorption spectrum of AuNPs capped with DS9 deposited onto a functionalized quartz slide.

(coverage percentage around 60%). The enhanced homogeneity in this sample is spectroscopically confirmed by the more defined and distinct absorption band at 560 nm in Figure 11 (solid line), although the 35 nm red shift with respect to the corresponding spectrum of Figure 7b indicates that also in this case a remarkable degree of particle aggregation occurs.

It is evident that the two films look very different. That organic-capped metallic systems exhibit remarkable differences in aggregation and adherence to glass surfaces is well-known.[40] These differences mainly arise from the chemical surface properties of the coating surfactants, that is from the nature of the corresponding end-groups. As the length and functionality of the terminal chain distinguish CDS9 and DS9, the data presented here agree with this finding, but the role played by the original morphology of the nanoclusters in determining the general characteristics of the resulting films cannot be disregarded. In addition, it is likely that the much slower solvent evaporation in the DS9-derivatized film procedure could favor a more regular disposition of the NPs onto the substrate.

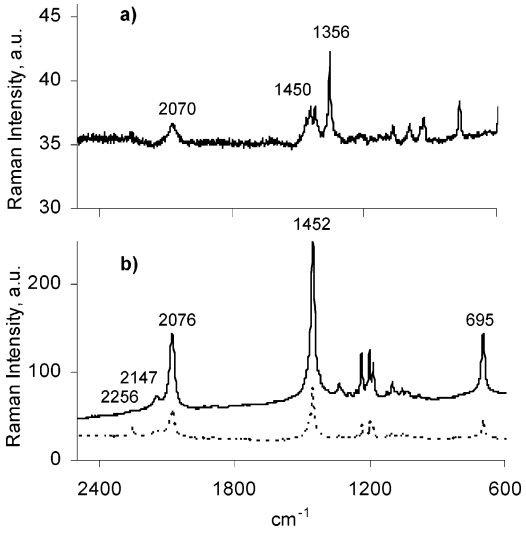

Figure 12. (a) SERS spectra of a 3D-SAM of polyCDS9 chemisorbed on gold nanoparticles after 7 min of UV irradiation (Au absorption background subtracted). Substrate: MPTS-functionalized glass slide. (b) SERS spectra of 3D-SAM of polyDS9 chemisorbed on gold nanoparticles before (dotted lined) and after 7 min of UV irradiation (solid line). Substrate: MPTS-functionalized quartz slide. Laser excitation at 633 nm.

After UV irradiation at different times, both samples did not show any noticeable change in optical images and in electronic spectra (data not shown), but the photopolymerization of the exposed diacetylene shells could be monitored by SERS technique. In Figure 12a the SERS spectrum of a film of CDS9-coated NPs after 7 min of UV irradiation is reported. In the high-frequency region, only the very weak signal at 2070 cm^{-1} is observed, typical of the C≡C stretching in blue polydiacetylenes. Weak spectral features in the C═C frequency region at 1445 and 1422 cm^{-1} are present, that can be assigned to the C═C stretching of the blue form and to the CH_2 bending mode, respectively. The sharper and more intense signal at 1356 cm^{-1} can be attributed to the double-bond stretchings of the carbazole rings. The peaks below 1300 cm^{-1} are not conclusively assigned in the literature and will not be discussed.

The SERS spectra of a film of DS9-protected gold nanoclusters measured before (dotted line) and after (solid line) UV exposure are reported in Figure 12b. The spectra look intense and with well-resolved peaks owing to the high homogeneity of the sample. The sharp signals at 2076 and 1452 cm^{-1}, typical of the blue form of polydiacetylenes, are well recognizable also in the nonirradiated sample, indicating that this system easily polymerizes even at white light exposure. Nevertheless, spontaneous polymerization turned out to be not complete, as shown by the presence of the weak peak at 2256 cm^{-1} corresponding to the triple-bond stretching of the monomer. After irradiation, the monomer signal disappears, while the other two peaks become more intense without significant changes in shape and position. Notice the presence of the 695 cm^{-1} signal, that was ascribed to a bending mode of the backbone[13] and could not be detected in Figure 12a because of the low spectrum intensity. Note also that the shoulder at 2147 cm^{-1} can probably be assigned to the overtone of the 1452 and 695 cm^{-1} modes. Also in this case, signals in the low-energy region, most likely due to collective stretching and bending modes of the conjugated skeleton, will not be discussed here.

On the whole, the SERS spectra of 2D- and 3D-SAM of polymerized CDS9 chemisorbed on gold show similarities and differences. First of all, the presence of carbazole and of conjugated backbone signals as well as the higher intensity of the C═C peak with respect to the C≡C one are common to both samples, although the peak profiles in the double-bond region appear sharper and more resolved in the CDS9-coated AuNP film. Since these evidences are consistent with the assembly architecture of Figure 4, it is likely that not only 2D-SAM but also 3D-SAM of polyCDS9 assume the same type of geometrical arrangement. On the other hand, for the monolayer chemisorbed on flat gold surface no signals of the blue-phase polymer were found despite the resonance conditions, while only this form was detected in the 3D film. These results indicate that, notwithstanding the steric hindrance of carbazole substituents, blue polyCDS9 can be obtained if the appropriate monolayer geometry is realized. This holds also for the SAMs of the more easily polymerizable DS9.

It is evident that for both diacetylenes the 3D- and the 2D-monolayers principally differ in the polymerization degree. An explanation for this behavior was offered in the case of dodecanethiolate monolayers, where the assembly differences were related with the concentration of surface sites and with the radius curvature, both larger for a 3D-SAM.[22] According to the authors, the increment of the two factors leads to a larger coverage of the Au surface and a change in the chain density over the length of the alkyl chains, with a resulting potential for the enhanced mobility of the outermost chain region and/or for lateral chain folding. On this basis, CDS9 and DS9 samples are also supposed to be affected in their morphology and reactivity by the topology and geometry of the metal core. Thus it is very likely that, in the polymerization process, the possibility of a better end-group accommodation for a 3D respect to a 2D monolayer, and so in particular for CDS9, may favor a more extended conjugation, as experimentally verified.

The results obtained here show that deposited films of capped AuNPs originate more ordered structures than when the monomer is chemisorbed on layers of preformed gold nanoclusters.[20]

Conclusions

The self-assembled monolayers (SAMs) of two different disulfides employed, whose main chemical difference consists in the substitution of the terminal seven-carbon chain of DS9 with the carbazolyl group of CDS9, were fabricated in two- and three-dimensional arrangement by monomer chemisorption on both gold rough platforms and on gold nanosized clusters (AuNPs).

Diacetylene-capped gold colloids of different size and shape were prepared by direct synthesis in organic solvent and characterized by TEM analysis. For DS9-coated AuNPs a quite narrow size distribution with an average diameter of 7.5 nm was found. For CDS9-protected AuNPs a wider dispersion in size and shape was obtained, characterized by a bimodal diameter distribution centered at 4.5 and 21 nm.

The monolayers photopolymerization investigated by means of SERS technique showed that both monomers, despite their different chemical structure, behave similarly in the same conditions. In fact, only the less extended red polymeric form was detected on flat platforms, while only the "more conjugated" blue phase was present in the SAMs of nanoparticle films. These results may be explained by considering the topological characteristics of the metal substrate as the key factor in the diacetylene polymerization process and the consequent larger surface coverage possible on spherical clusters relative to that of flat platforms.[41,42]

Finally, we would like to stress that the incorporation of photopolymerizable diacetylene groups within the monolayer alkyl chains can lead to stable and robust organic/metal architectures which present unique linear and nonlinear optical properties, connected to the highly conjugated polydiacetylene backbone. The presence of carbazolyl substituents is expected to improve nonlinearity as well as photoconductivity of these hybrid materials.

Acknowledgment. This paper is dedicated to the memory of Professor Carlo Dell'Erba, who first projected and synthesized the CDS9 molecule. Thanks are also due to Dr. Maria Maddalena Carnasciali and Professor Maurizio Muniz-Miranda for their help in the Raman measurements, to Dr. Massimo Maccagno and Dr. Carlo Scapolla for their aid in NMR and MS determinations, and to Dr. Valeria Rocca and Mr. Andrea Galatini for their help in HLPC measurements. Financial support from the Italian FIRB "Molecular and Organic/Inorganic Hybrid Nanostructures for Photonics" (Contract No. RBNE01P4JF) is acknowledged.

Appendix

Synthesis of CDS9. *Materials and Methods.* "Petroleum ether" and "light petroleum" refer to the fractions boiling in the range of 40−60 °C and 80−110 °C, respectively. Solvents used as eluents were distilled prior to use. *N*,*N*-Dimethylformamide (DMF), ethanol, and light petroleum were extra pure commercial products and were used as received. Anhydrous methylene chloride was syringed under argon. Pyridine was twice distilled prior to use, first from KOH pellets and then from CaH_2. 9*H*-Carbazole (**1**), propargyl bromide (80% w/w in toluene, 8.9 M), 10-undecyn-1-ol (**4**), and tosylchloride were commercial products used as received.

Copper(I) chloride was prepared as follows. A solution of Na_2SO_3 (77.3 g, 0.61 mol) and NaOH (24.5 g, 0.61 mol) in deionized water (750 mL) was slowly dropped under efficient stirring into a solution of $CuSO_4 \cdot 5H_2O$ (306.5 g, 1.23 mol) and NaCl (80.2 g, 2.09 mol) in deionized water (1.1 L). The resulting white precipitate was filtered from the blue-cobalt solution, washed with deionized water, ethanol, and diethyl ether, and stored under argon (85.3 g, yield 70.2%).

Synthetic Procedure (According to Scheme 1 in the Text). *9-(Prop-2-ynyl)-9H-carbazole (2).* 9*H*-Carbazole (**1**; 16.53 g, 98.86 mmol) was dissolved in warm toluene (636 mL). The solution was left to cool slowly until the saturation temperature was reached and then propargyl bromide (16.7 mL of a commercial 80% w/w solution in toluene, 148.29 mmol), tetrabutylammonium iodide (1.59 g, 4.94 mmol), and 50% aqueous NaOH (63.7 mL) were added. The flask was sonicated for 15 h, keeping the temperature below 50 °C. The mixture was then acidified to pH 1 by adding 37% HCl, diluted with water, and extracted with Et_2O. The organic layer was washed to neutrality with water and then dried over Na_2SO_4. Evaporation of the solvent gave a residue which was flash-chromatographed on a silica gel column using as eluents petroleum ether/dichloromethane mixtures of varying composition. The resulting yellow-orange residue was recrystallized from light petroleum, yielding 19.5 g (96%) of **2** as white crystals, mp 107.0−107.7 °C (lit.[43]108 °C). ^{1}H NMR (DMSO-d_6, ppm): δ 3.25 (t, J = 2.2 Hz, 1H,), 5.32 (d, J = 2.6 Hz, 2H), 7.24 (t, J = 7.6 Hz, 2H), 7.49 (td, J = 1.2 and 7.6 Hz, 2H,), 7.69 (d, J = 8.0 Hz,

2H), 8.17 (d, $J = 7.8$ Hz, 2H). ^{13}C NMR ($CDCl_3$, ppm): δ. 32.29, 72.23, 77.82, 108.72, 119.59, 120.44, 123.28, 125.90, 139.84.

*9-(3-Iodoprop-2-ynyl)-9H-carbazole (**3**).* Compound **2** (7.45 g, 36.29 mmol) was introduced into a two-necked flask equipped with a thermometer and a dropping funnel, and the system was placed under argon. THF (400 mL) was added, and the resulting clear solution was cooled to 0 °C and kept under magnetic stirring while adding *n*-BuLi (30 mL of a 1.5 M solution in hexane, 43.55 mmol). After 40 min, iodine (14.3 g, 54.41 mmol) was added, and the resulting dark-red solution was allowed to react for 4.5 h. The excess iodine was then destroyed with a 5% sodium sulfite solution, the resulting colorless solution was diluted with water, and then repeatedly extracted with ethyl ether. After drying with anhydrous sodium sulfate, rotoevaporation of the organic solution gave a dark-brown residue which was recrystallized from toluene. The resulting brown solid (10.82 g, 90%) melted at 135.4−136.8 °C.

^{1}H NMR ($CDCl_3$, ppm): δ 5.17 (s, 2H), 7.23−7.31 (m, 2H), 7.44−7.50 (m, 4H), 8.10 (d, $J = 7.6$ Hz, 2H). ^{13}C NMR (DMSO-d_6, ppm): δ 32.24, 66.49, 74.90, 109.33, 119.47, 120.29, 122.43, 125.86, 139.37. MS (EI) *m*/*z*: 331 [M^+]. Anal. Calcd for $C_{15}H_{10}IN$: C, 54.42; H, 3.04; N, 4.23. Found: C, 54.33; H, 3.05; N, 4.19.

*Cu(I) Salt of 10-Undecyn-1-ol (**5**).* A solution of 10-undecyn-1-ol (**4**; 16.5 mL, 85.89 mmol) in ethanol (200 mL) was slowly added under efficient stirring to a solution of freshly prepared CuCl (85.01 g, 858.69 mmol) in 12 N NH_3 (3.5 L) containing some hydroxylamine hydrochloride. After completion of the addition, stirring was continued for 90 min while small aliquots of hydroxylamine hydrochloride were added portionwise; the yellow precipitate formed was then filtered and washed in sequence with water, ethanol, and diethyl ether, yielding **5** as a yellow powder (17.88 g yield 90.2%). Anal. Calcd for $C_{11}H_{19}$-CuO: C, 57.24; H, 8.30. Found: C, 57.14; H, 8.18.

*14-(9H-9-Carbazolyl)tetradeca-10,12-diyn-1-ol (**6**).* A slurry of **5** (14.6 g, 63.3 mmol) in dry pyridine (227 mL) was warmed to 40 °C under argon. To the resulting yellow suspension a solution of **3** (19.1 g. 57.7 mmol) in dry pyridine (142 mL) was added over a period of 40 min. After standing for further 20 h at room temperature, the mixture was cooled by addition of crushed ice, poured into an excess (1.2 L) of concentrated hydrochloric acid, diluted with water, and the aqueous solution was extracted with ethyl ether. After separation, the organic layer was washed with 5% HCl, water, and dried over anhydrous sodium sulfate. Evaporation of the solvent gave a residue which was purified by flash chromatography (silica gel column; eluent dichloromethane/diethyl ether (10:1). Recrystallization from light petroleum finally gave 7.12 g (yield 33.3%) of a white solid, mp 84.0−85.1 °C. ^{1}H NMR ($CDCl_3$, ppm): δ 1.26−1.58 (m, 14H), 2.18 (t, $J = 7.0$ Hz, 2H,), 3.60 (t, $J = 6.6$ Hz, 2H), 5.10 (s, 2 H), 7.26−7.30 (m, 2H), 7.47−7.50 (m, 4H,), 8.09 (dd, $J = 0.8$ and 7.6 Hz, 2H,) (the OH proton rapidly exchanges with the solvent). ^{13}C NMR (DMSO-d_6, ppm): δ 18.12, 25.37, 27.35, 28.07, 28.27, 28.79, 32.31, 32.45, 60.52, 60.64, 64.15, 67.68, 71.85, 81.07, 109.40, 119.43, 120.29, 122.47, 125.84, 139.47. MS (EI) *m*/*z*: 371 [M^+]. Anal. Calcd for $C_{26}H_{29}NO$: C, 84.06; H, 7.87; N, 3.77. Found: C, 83.88; H, 7.66; N, 3.69.

*14-(9H-9-Carbazolyl)tetradeca-10,12-diyn-1-yl p-Toluenesulfonate (**7**).* Dry pyridine (3.7 mL) was added to a magnetically stirred solution of **6** (4.29 g, 11.55 mmol) in dry CH_2Cl_2 (172 mL) which was then cooled to 10 °C and added with *p*-tosylchloride (3.65 g, 17.32 mmol) in small portions. After standing for an additional 10 min at the same temperature the mixture was allowed to reach room temperature, left under stirring for 40 h, poured into a mixture of 37% HCl (42 mL) and crushed ice, and finally extracted with ethyl ether. The organic layer was washed repeatedly with water, dried over anhydrous sodium sulfate, and the solvent was removed under reduced pressure to give a residue which was flash-chromatographed on a silica gel column (eluent: dichloromethane/petroleum ether mixtures of varying compositions). After washing with boiling petroleum ether, the crude product from the chromatographic separation yielded 4.88 g (80%) of an orange oil which was not further purified.

^{1}H NMR ($CDCl_3$, ppm): δ 1.18−1.56 (m, 14H), 2.19 (t, $J = 7.0$ Hz, 2H), 2.42 (s, 3H), 3.99 (t, $J = 6.6$ Hz, 2H), 5.09 (s, 2 H), 7.25−7.34 (m, 4H), 7.46−7.49 (m, 4H), 7.77 (d, $J = 8.4$ Hz, 2H), 8.09 (dd, $J = 1.2$ and 7.6 Hz, 2H). ^{13}C NMR (DMSO-d_6, ppm): δ 18.09, 20.95, 24.52, 27.29, 27.97, 28.10, 28.45, 32.30, 64.15, 67.65, 70.75, 71.87, 81.05, 109.40, 119.43, 120.29, 122.46, 125.83, 127.45, 130.01, 132.43, 139.45, 144.69 (two signals are missing, possibly due to insufficient resolution or to isochromism). MS (ESI) *m*/*z*: 526.2 ($M + H^+$), 548.2 ($M + Na^+$), 564.2 ($M + K^+$). Anal. Calcd for $C_{33}H_{35}NO_3S$: C, 75.40; H, 6.68, N, 2.26; S, 6.10. Found: C, 75.33; H, 6.82; N, 2.20; S, 6.15.

*14-(9H-9-Carbazolyl)-1-iodotetradeca-10,12-diyne (**8**).* To a solution of **7** (4.88 g, 9.28 mmol) in acetone (160 mL) a solution of sodium iodide (2.78 g, 18.56 mmol) in acetone (40 mL) was added under magnetic stirring at room temperature over a period of 66 h. The mixture was then diluted with water (1.5 L) and extracted with Et_2O. The organic layer was washed twice with water and dried over Na_2SO_4. Evaporation of the solvent gave a yellow residue which was recrystallized from ethanol to yield 3.07 g (68.7%) of **7** as a white solid, mp 84.9−85.5 °C.

^{1}H NMR ($CDCl_3$): δ 1.26−1.56 (12 H, m), 1,79 (2 H, quin *J* 7.2), 2.20 (2 H, t, *J* 7.0), 3.16 (2 H, t, *J* 67.2), 5.11 (2 H, s), 7.24−7.31 (2 H, m), 7.47−7.50 (4 H, m), 8.09 (2 H, dd, *J* 1.2 and 7.6). ^{13}C NMR (DMSO-d_6): δ 8.98, 18.10, 27.29, 27.64, 27.97, 28.13, 28.50, 29.66, 32.31, 32.73, 64.14, 67.65, 71.87, 81.08, 109.41, 119.43, 120.29, 122.45, 125.84, 139.45. MS (EI) *m*/*z*: 481 [M^+]. Anal. Calcd for $C_{26}H_{28}IN$: C, 64.87; H, 5.86; N, 2.91. Found: C, 64.71; H, 6.02; N, 2.80.

*14-(9H-9-Carbazolyl)tetradeca-10,12-diyn-1-yl Thioacetate (**9**).* Compound **8** (1.90 g, 3.95 mmol) was added under magnetic stirring to a solution of potassium thioacetate (0.5 g, 4.34 mmol) in *N*,*N*-dimethylformamide (46 mL). The mixture was stirred at room temperature for 24 h, then poured into 200 mL of diluted (4%) HCl and extracted with diethyl ether, the organic layer was repeatedly washed with water, and dried over anhydrous sodium sulfate. Evaporation of the solvent gave a yellow residue which was recrystallized from light petroleum to yield 1.31 g (77.2%) of **9** as a whitish solid, mp 104.3−105.5 °C.

^{1}H NMR ($CDCl_3$, ppm): δ 1.24−1.56 (m, 14 H), 2.19 (t, $J = 7.0$ Hz, 2H), 2.31 (s, 3H,), 2.84 (t, $J = 7.2$ Hz, 2H,), 5.09 (s, 2H), 7.25−7.27 (m, 2H,), 7.46−7.49 (m, 4H,), 8.09 (d, $J = 7.6$ Hz, 2H,). ^{13}C NMR (DMSO-d_6, ppm): δ 18.10, 27.31, 27.95, 28.00, 28.17, 28.22, 28.27, 28.54, 28.97, 30.45, 32.31, 64.14, 67.67, 71.85, 81.06, 109.40, 119.42, 120.29, 122.46, 125.82, 139.46, 195.19. MS (EI) *m*/*z*: 430 [M^+]. Anal. Calcd for $C_{28}H_{31}$-NOS: C, 78.28; H, 7.27; N, 3.26; S, 7.46. Found: C, 78.32; H, 7.16; N, 3.23; S, 7.38.

14-(9H-9-Carbazolyl)tetradeca-10,12-diyn-1-yl Disulfide (CDS9). A volume of 3 M KOH (30 mL) was slowly added under magnetic stirring to a solution of **9** (1.28 g, 2.98 mmol) in acetone (30.3 mL) under argon at room temperature. The

resulting mixture was kept under stirring for additional 20 h, then poured onto crushed ice and diluted HCl. The product was isolated with dichloromethane. The organic layer was washed thoroughly with water and dried over Na_2SO_4. The isolated dark-yellow solid was suspended in absolute ethanol (25 mL), and the mixture was stirred for 18 h at room temperature. The yellowish solid recovered after filtration was recrystallized from light petroleum, thus obtaining 803 mg (yield 35%), mp 113.8−114.6 °C.

^{1}H NMR ($CDCl_3$ ppm): δ 1.24−1.67 (m, 2H,), 2.19 (t, J = 7.0 Hz, 4H,), 2.65 (t, J = 7.2 :, 4H), 5.09 (s, 4H), 7.23−7.30 (m, 4H), 7.46−7.49 (m, 8H), 8.09 (dd, J = 1.2 and 7.6, 4H). ^{13}C NMR ($CDCl_3$, ppm): δ 19.14, 28.00, 28.44, 28.72, 28.94, 29.11, 29.16, 29.25, 33.00, 39.14, 64.44, 69.03, 69.74, 80.87, 108.72, 119.60, 120.43, 123.27, 125.93, 139.83. HRMS (ESI − q-TOF) m/z: 773.3968 ($M + H^+$). Calculated mass for $C_{52}H_{57}N_2S_2$: 773.3958. Anal. Calcd for $C_{52}H_{57}N_2S_2$: 80.78; H, 7.30; N, 3.62; S, 8.29. Found: C,80.66; H, 7.34; N, 3.49; S 8.20.

Supporting Information Available: Figures showing the HPLC trace of the CDS9 monomer, the ^{1}H and ^{13}C NMR spectra of CDS9 and its synthetic intermediates, as well as TEM and spectroscopic data for dodecanethiol-capped Au clusters. The material is available free of charge via the Internet at http://pubs.acs.org.

References and Notes

(1) Kobayashi, T. *Primary Photoexcitations in Conjugated Polymers*; Sariciftci, N.S., Ed.; World Scientific: Singapore, 1996; Chapter 15.

(2) Comoretto, D.; Moggio, I.; Alloisio, M.; Cuniberti, C.; Musso, G. F.; Ottonelli, M.; Dellepiane, G.; Kajzar, F.; Lorin, A. *Opto−Electron. Rev.* **1999**, *7*, 121.

(3) Mort, J., Pfister, G., Eds. *Electronic Properties of Polymers*; Wiley: New York, 1982.

(4) Bisburg, J.; Curming, W. J.; Gaerdiana, R. A.; Hutchinson, K. D.; Ingwel, R. I.; Kolb, E. S.; Mehta, P. G.; Mimms, R. A.; Peterson, L. P. *Macromolecules* **1995**, *28*, 386.

(5) Law, K. Y. *Chem. Rev.* **1993**, *93*, 449.

(6) Menzel, H.; Horstman, S.; Mowery, M. D.; Cai, M.; Evans, C. E. *Polymer* **2000**, *41*, 8113 and references therein.

(7) Kim, T.; Chan, K. C.; Crooks, R. M. *J. Am. Chem. Soc.* **1997**, *119*, 189 and references therein.

(8) Giorgetti, E.; Margheri, G.; Sottini, S.; Chen, X.; Cravino, A.; Comoretto, D.; Cuniberti, C.; Dell'Erba, C.; Dellepiane. G. *Synth. Met.* **2000**, *115*, 257.

(9) Giorgetti, E.; Margheri, G.; Gelli, F.; Sottini, S.; Comoretto, D.; Cravino, A.; Cuniberti, C.; Dell'Erba, C.; Moggio, I.; Dellepiane, G. *Synth. Met.* **2001**, *116*, 129.

(10) Margheri, G.; Giorgetti, E.; Sottini, S.; Toci, G. *J. Opt. Soc. Am. B* **2003**, *20*, 731.

(11) Giorgetti, E.; Margheri, G.; Sottini, S.; Toci, G.; Muniz-Miranda, M.; Moroni, L.; Dellepiane, G. *Phys. Chem. Chem. Phys.* **2002**, *4*, 2762.

(12) Bozhevolnyi, S. I.; Ereland, J.; Leosson, K.; Skovgaard, P. M. W.; Hvam, J. M. *Phys. Rev. Lett.* **2001**, *86*, 3008.

(13) Bloor, D.; Preson, F. H.; Ando, D. J.; Batchelder, D. N. *Structural Studies of Macromolecules by Spectroscopic Methods*; Iven, K. J., Ed.; John Wiley and Sons: London, 1976.

(14) Batchelder, D. N.; Bloor, D. *Advances in Infrared and Raman Spectroscopy*; Clark, R. J. H., Hester, R. E., Eds.; Wiley Heydon: London, 1984.

(15) Ulman, A. *Chem. Rev.* **1996**, *96*, 1533.

(16) Dubois, L. H.; Nuzzo, R. G. *Annu. Rev. Phys. Chem.* **1992**, *43*, 437.

(17) Bain, C. D.; Whitesides, G. M. *Angew. Chem., Int. Ed. Engl.* **1989**, *28*, 506.

(18) Brust, M.; Walker, M.; Bethell, D.; Schiffrin, D. J.; Whyman, R. *J. Chem. Soc., Chem. Commun.* **1994**, 801.

(19) Zhou, H. S.; Wada, T.; Sasabe, H. *J. Chem. Soc., Chem. Commun.* **1995**, 1525.

(20) Menzel, H.; Mowery, M. D.; Cai, M.; Evans, C. E. *Adv. Mater.* **1999**, *11*, 131.

(21) Mowery, M. D.; Evans, C. E. *Tetrahedron Lett.* **1997**, *38*, 11.

(22) Hoestetler, M.; Wingate, J. E.; Zhong, C. J.; Harris, J. E.; Vachet, R. W.; Clark, M. R.; Londono, J. D.; Green, S. J.; Stokes, J. J.; Wignall, G. D.; Glish, G. L.; Porter, M. D.; Evans, N. D.; Murray, R. W. *Langmuir* **1998**, *14*, 17 and references therein.

(23) Giorgetti, E.; Muniz-Miranda, M.; Margheri, G.; Giusti, A.; Sottini, S.; Alloisio, M.; Cuniberti, C.; Dellepiane, G. *Langmuir* **2006**, *22*, 1129.

(24) Giorgetti, E.; Muniz-Miranda, M.; Giusti, A.; Delrosso, T.; Dellepiane, G.; Margheri, G.; Sottini, S.; Alloisio, M.; Cuniberti, C. *Thin Solid Films* **2006**, *459*, 36.

(25) Menzel, H.; Mowery, M. D.; Cai, M.; Evans, C. E. *J. Phys. Chem. B* **1998**,*102*, 9550.

(26) Cavalleri, O.; Prato, M.; Chincarini, A.; Rolandi, R.; Canepa, M.; Gliozzi, A.; Alloisio, M.; Lavagnino, L.; Cuniberti, C.; Dell'Erba, C.; Dellepiane, G. *Appl. Surf. Sci.* **2005**, *246*, 403.

(27) Doty, R. C.; Tshikhudo, T. R.; Brust, M.; Fernig, D. G. *Chem. Mater.* **2005**, *17*, 4630 and references therein.

(28) Leff, D. V.; Ohara, P. C.; Hearth, J. R.; Gelbart, W. M. *J. Phys. Chem.* **1995**, *99*, 7036.

(29) Bohren, C. F.; Huffman, D. R. *Absorption and Scattering of Light by Small Particles*; John Wiley: New York, 1983.

(30) Feldheim, D. L., Foss, C. A., Eds. *Metal Nanoparticles Synthesis, Characterization and Applications*; Marcel Dekker: New York, 2002.

(31) Yu, Y. Y.; Chang, S. S.; Lee, C. L.; Wang, C. R. C. *J. Phys. Chem. B* **1997**, *101*, 6661.

(32) Kamat, P. V.; Flumiani, M.; Dawson, A. *Colloids Surf., A* **2002**, *202*, 269 and references therein.

(33) Link, S.; Beeby, A.; FitzGerald, S.; El-Sayed, M. A.; Schaaff, T. G.; Whetten, R. L. *J. Phys. Chem. B* **2002**, *106*, 3410.

(34) Huang, T.; Murray, R. W. *J. Phys. Chem. B* **2001**, *105*, 12498.

(35) Wilcoxon, J. P.; Martin, J. E.; Parsapour, F.; Wiedenman, B.; Kelley, D. F. *J. Chem. Phys.* **1998**, *108*, 9137.

(36) Mooradian, A. *Phys. Rev. Lett.* **1969**, *22*, 185.

(37) Zheng, J.; Petty, J. T.; Dickson, R. M. *J. Am. Chem. Soc.* **2003**, *125*, 7780.

(38) Shen, X. C.; Jiang, L. F.; Liang, H.; Lu, X.; Zhang, L.-j.; X-Yan Liu, J. *Talanta* **2006**, *69*, 456 and references therein.

(39) Johnson, S. R.; Evans, S. D.; Brydson, R. *Langmuir* **1998**, *14*, 6639 and references therein.

(40) Cañamares, M. V.; Garcia-Ramos, J. V.; Gomez-Varga, J. D.; Domingo, C.; Sanchez-Cortes, S. *Langmuir* **2005**, *21*, 8546.

(41) Templeton, A. C.; Wuelfing, W. P.; Murray, R. W. *Acc. Chem. Res.* **2000**, *33*, 27.

(42) Demers, L. M.; Mirkin, C. A.; Mucic, R. C.; Reynolds, R. A.; Letsinger, R. L.; Elghanian, R.; Viswanadham, G. *Anal. Chem.* **2000**, *72*, 5535.

(43) Broggini, G.; Bruche, L.; Zecchi, G.; Pilati, T. *J. Chem. Soc., Perkin Trans. 1* **1990**, 533−539.